Electronics and Electrical Engineering

AIMS Electronics and Electrical Engineering, 6(2): 144–160.
DOI: 10.3934/electreng.2022009
Received: 02 January 2022
Revised: 18 March 2022
Accepted: 22 March 2022
Published: 31 March 2022

http://www.aimspress.com/journal/ElectrEng

Research article

Islanding detection in utility grid with renewable energy using rate of change of frequency and signal processing technique

Om Prakash Mahela[1], Pappu Ram Bheel[2], M.K. Bhaskar[2] and Baseem Khan[3,*]

[1] Power System Planning Division, Rajasthan Rajya Vidhyut Prasaran Nigam Ltd., Jaipur, India
[2] M.B.M. Engineering College, Jai Narain Vyas University Jodhpur (Rajasthan), India
[3] Department of Electrical and Computer Engineering, Hawassa University, Hawassa, Ethiopia, 05

*** Correspondence:** Email: baseem.khan04@gmail.com.

Abstract: This manuscript has introduced an algorithm based on current signals and frequency rate change (ROCOF) to identify islanding events. Current is analyzed by the use of Stockwell transform (ST) at 3.84 kHz sampling frequency (SF) and a median of absolute values of every column of output matrix (CSIRI) is computed. Rate of change of CSIRI (ROCOCSIRI) is computed. Proposed current based islanding recognition index (IRIC) is computed by multiplying ROCOF with CSIRI & ROCOCSIRI and a weight factor (WC). Threshold values THI1 & THI2 are selected 100 and 3000 for IRIC for identifying the Islanding condition. These are also effective to differentiate islanding conditions from non-islanding events which include both the faulty and operational events. Magnitude of IRIC is greater than 3000 for the faulty events and lower than 100 for operational events. For islanding events magnitude of IRIC falls in between the 100 and 3000. Algorithm is effective to identify and classify the events in three categories which are islanding events, faulty events and operational events effectively. Study is realized in MATLAB/Simulink scenario.

Keywords: current; frequency; islanding; renewable energy; Stockwell transform; utility grid

1. Introduction

Integration of Renewable energy (RE) plants to distribution network changes nature from

passive to active at fast rate. During the island mode of operation of part of grid, the RE plants continuously supply loads and remaining part of utility grid is disconnected. Islanding is the event when distribution network is disconnected from utility grid. It is expected that islanding is recognized in minimum time and RE generators are disconnected from distribution system. This will ensure the safety of operation and maintenance (O&M) staff of the utility as well as power plants. Islanding creates instable frequency and voltage which also cause damage to equipment. IEEE 1547 and UL 1741 standards states that RE plants required to be disconnected from grid network in a time period of 2s after occurrence of Islanding. Islanding detection methods (IDMs) are categorized in local IDM and remote IDM. A communication channel is employed by the remote IDMs between utility network and RE plant [1,2]. Decisions of local IDMs are based on the measurements taken location of RE plant. Local IDMs are categorized in passive IDM and active IDM. Passive IDMs use estimation of system parameters such as frequency and voltage at point of common coupling (PCC) to detect islanding. These IDMs has large time for estimation of events, and large non-detection zone (NDZ). The problem of NDZ can be obviated by the use of signal processing techniques which are effective for tracking changes in system parameters even of small magnitude [3,4]. In [5], authors introduced a Multi-gene Genetic Programming (MGP) supported technique for detection of islanding events of DG sources. MGP effectively uses mathematical and logic functions for detecting and classifying the islanding phenomenon to high accuracy. This method used twelve parameters which increased the computational complexity. In [6], authors suggested a hybrid mechanism for islanding identification for DG sources. It is designed by combining Random Forest (RF) with Moth Flame Optimization (MFO) approaches and combined approach is designated as RFMFO. It has main objective to minimize the Non-Detective Zone (NDZ) and it has been reduced to zero. However, performance of method is reduced when there is imbalance between the generation of RE generators and load in the micro-grid. In [7], authors introduced a method which is effective to classify a set of different parameters of power system using sensitivity which is considered a preliminary step in choosing the suitable parameter to identify the islanding event. Hence, islanding identification is achieved using dilated parameters of reactive power and also differentiated islanding from other grid disturbances. This method may give false signals when there is heavy mismatch of the reactive power. In [8], a method for islanding recognition with the help of features extracted from reactive power applying the Empirical Mode Decomposition (EMD) is introduced. This approach is efficient in identifying islanding in a time interval lower compared to two cycles. A detailed analysis of different conventional and intelligent methods of islanding detection is presented in [9]. Advantages, disadvantages and a summary to compare existing islanding detection methods are discussed in detail. In [10], authors reviewed the Islanding detection methods with main focus on the islanding detection techniques based on active methods. Further, authors also discussed the reduction of the islanding detection sensitivity due to presence of multiple distributed generation (DG) sources. In [11], authors presented a detailed survey of the islanding detection techniques (IDTs) for identifying the advantages and disadvantages of these techniques. Authors also designed a machine-learning strategy supported by signal processing techniques to overcome the demerits of existing IDTs. Proposed method achieved the 97.2% training accuracy and 100 % testing accuracy in islanding identification time of 25 *ms.* In [12], authors introduced a optimal voltage control (OVC) system based on the Lyapunov theory for islanded micro-grids (MGs) to effectively control the distributed generation (DG) resources using their primary level controllers. This method is effective to minimize the power losses and voltage deviations. In [13], authors designed a multilevel inverters

(MLIs) circuit having capability of cascaded connection to improve structure for grid connected DGs. This inverter provides transformer less connection of DG resources to network. Designed control system effectively minimizes the harmonics of output current.

After detailed analysis of literature discussed in the above paragraph, it is observed that performance of passive IDMs can be improved by hybridization of signal processing techniques and rate of change of system parameters. This has been considered as key investigation for the research work undertaken in this paper and following are main contributions of this paper:

- An IDM based on processing of current signals using ST and ROCOF to identify islanding events is proposed in this paper.
- A current based islanding recognition index (IRIC) is designed which is computed by processing the current signals using ST and ROCOF. Threshold values THI1 & THI2 are used for identifying the Islanding condition and discriminating the islanding conditions from non-islanding events.
- Proposed IDM is effective to identify and classify the events in three categories which are islanding events, faulty events and operational events effectively.

Seven sections are used to structure the paper. Literature review, research gaps and research contributions are discussed in the section 1. Test system used for the study is elaborated in section 2. Proposed current based IDM is described in section 3. Simulation results have been discussed in the section 5. Comparison of the performance of proposed IDM with the IDMs reported in literature is included in section 6. Research work is concluded in the section 7.

2. Test system

All the investigated events have been simulated on IEEE-13 buses test network which is taken as distribution-grid where wind power plant (WPP) and solar power plant (SPP) are integrated. This network is operated at 60 Hz and 5 MVA. Feeders & loads are operating at voltage levels of 4.16 kV & 0.48 kV. Details of load quantum and capacitors which are being connected to this network are available in [14]. Further, a WPP rated at 1.5 MW and a SPP rated at 1 MW are interfaced on junction 680 of network as explained in Figure 1. Hence, junction 680 is considered as PCC for the purpose of grid integration of RE plants. WPP is designed considering a double fed induction generator (DFIG) which is interfaced to network using a transformer (GT-WPP). Details of WPP available in [15] have been used in this study. A SPP using photovoltaic (PV) and rated at 1 MW is interfaced to junction 680 of network through a transformer (GT-SPP). Data of SPP available in [16] have been used for this study. A transformer (DT-feeder) is placed among junctions 633 and 634 for maintaining these nodes at 4.16 kV & 0.48 kV voltages sequentially. Test DS is integrated to large area power utility network through a transformer considered as Grid interconnecting transformer (ICT-Utility Grid). Details of voltage, MVA, winding inductance and winding resistance are available in [17]. Lengths of feeders are similar to original feeder and reported in [18,19]. A circuit breaker is placed between nodes 671 & 692. Islanding relay is placed at junction 650 where voltage and current are captured.

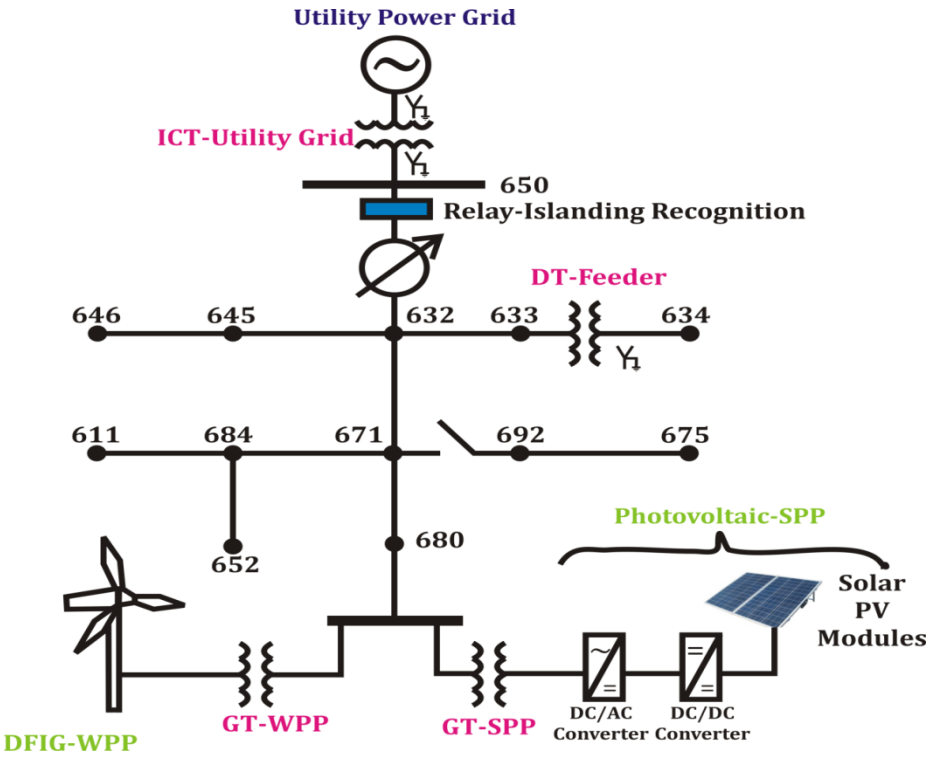

Figure 1. Test distribution grid interfaced with WPP and SPP.

3. Proposed current based IDM

A passive islanding detection method (IDM) based on processing of current signals using signal processing method and rate of change of frequency is proposed which is described with the help of below mentioned steps. A flow diagram of the proposed IDM is described in Figure 2.

- Record current waveform and frequency at node 650. Current signal and frequency are monitored continuously. Hence, proposed IDM continuously monitors the current and frequency in the real time scenario and detect islanding event as and when incident.
- Decompose current signal using ST at 3.84 kHz sampling frequency and output matrix is obtained. Take absolute values of every element of output matrix and labelled the output matrix with absolute values as STI. It is matrix with dimension 385 x 768.
- Calculate median of each column of STI and designate it as CSIRI using the below mentioned MATLAB codes. CSIRI is row matrix of the dimension 1 x 768. Different statistical operators such as variance, co-variance, summation, and standard deviations are tested, it is observed that results for islanding detection with median operator are superior.

$$CSIRI = median(STI)$$

- Compute the rate of change CSIRI (ROCOCSIRI) by differentiating the CSIRI with respect to time giving the ROCOCSIRI using the below mentioned MATLAB codes:

$$ROCOCSIRI = diff(CSIRI)$$

- Compute ROCOF by differentiating the frequency (F) with respect to time giving the ROCOF using the below mentioned MATLAB codes:

$$ROCOF = diff(F)$$

- Multiply element by element the CSIRI, ROCOCSIRI and ROCOF to compute the current islanding recognition index (IRIC) using as suitable weight factor (WC) as detailed below. Here weight factor is considered to be equal to 2 x 10^{12}. WC is an empirical value and selected by testing the IDM on 100 data set of islanding events and 100 data set of non-islanding events. These data set are obtained by changing the parameters such as frequency, angle of event incidence, loads, capacitor values etc. In general WC is not dependent on the system. However, it may be adjusted at the time of deployment of IDM in the grid depending on the RE generation level, if required:

$$IRIC = CSIRI \times ROCOCSIRI \times ROCOF \times WC$$

- Set the first threshold magnitude (THI1) equal to 100 for IRIC and select second threshold magnitude equal to 3000. These threshold magnitudes are empirical values and selected by testing the IDM on 100 data set of islanding events and 100 data set of non-islanding events. These data set are obtained by changing the parameters such as frequency, angle of event incidence, loads, capacitor values etc. If peak magnitude of IRIC is less compared threshold THI1 then the event is operational in nature whereas for the values of IRIC greater than threshold THI2 the event will be faulty in nature. For the islanding events the peak magnitude of IRIC will follow the relation: THI1 < IRIC < THI2.

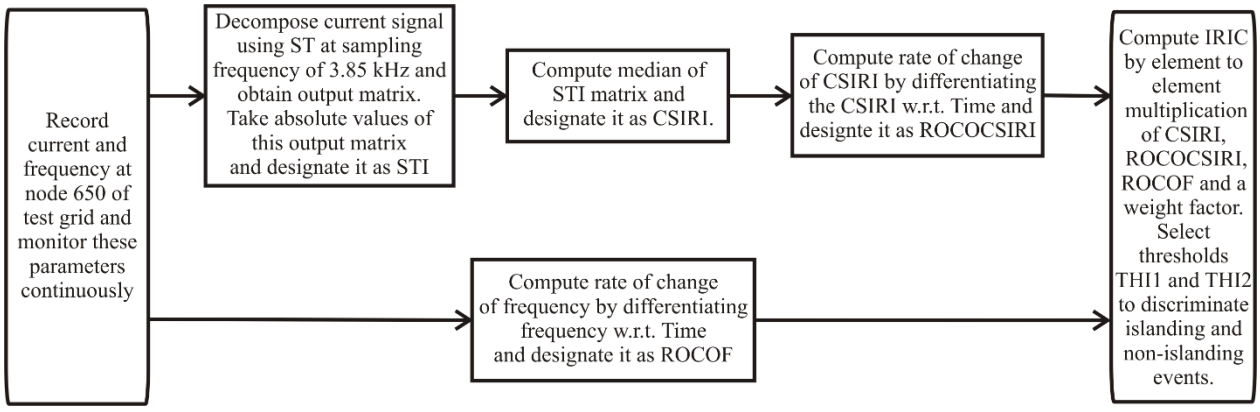

Figure 2. Flow process of proposed IDM.

4. Results of simulation and discussion

Simulation results obtained using the proposed current based IDM is discussed in this section.

A. Healthy condition

Test distribution grid having WPP & SPP is simulated for 0.2 s without any disturbance. Current waveform and frequency are recorded at junction 650 of grid and explained in Figure 3 (a) and (b) sequentially. Proposed CSIRI, ROCOF, ROCOCSIRI and IRIC are detailed Figure 3 (c), (d), (e) and (f) respectively.

Figure 3 (a) depicts that current magnitude is constant and any disturbance is not associated with the current. Figure 3 (b) describes that frequency is constant at all times of study. Magnitude of the CSIRI index is also constant as detailed in Figure 3 (c). Figure 3 (d) details that ROCOF is nearly zero. Figure 3(e) also describes that magnitude of the ROCOCSIRI is zero for the investigated time. Figure 3 (f) details that magnitude of IRIC is zero which is below the threshold THI1. This indicates that no event has incident on the test distribution grid.

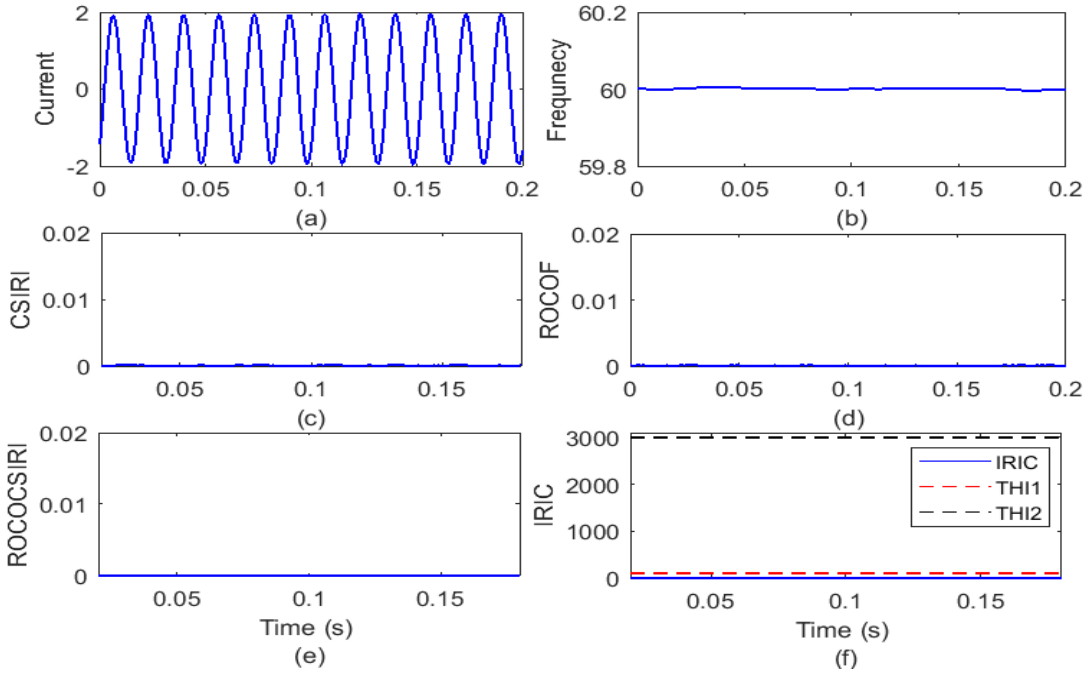

Figure 3. Test grid is operating in healthy condition (a) current signal (b) frequency (c) CSIRI (d) ROCOF (e) ROCOCSIRI (f) IRIC.

B. Islanding with availability of WPP and SPP

Test distribution grid having WPP & SPP is simulated for 0.2 s. Islanding event is simulated at 6^{th} cycle in the presence of both WPP and SPP by disconnecting the test distribution system from the utility grid network. Current waveform and frequency are recorded at junction 650 of grid and explained in Figure 4 (a) and (b) sequentially. Proposed CSIRI, ROCOF, ROCOCSIRI and IRIC are detailed Figure 4(c), (d), (e) and (f) respectively.

Figure 4 (a) depicts that current magnitude has decreased to zero at the time of occurrence of islanding with both WPP and SPP. Figure 4 (b) describes that frequency increases due to occurrence of islanding with WPP and SPP. Magnitude of the CSIRI index has increased with sharp peak at instant of islanding and remains low for all other times as detailed in Figure 4(c). Figure 4(d) details that ROCOF is nearly zero prior to occurrence of islanding and increases just after occurrence of islanding. Figure 4(e) also describes that magnitude of the ROCOCSIRI has increased with high magnitude peak and low for all other times. Figure 4 (f) details that magnitude of IRIC has increased due to occurrence of islanding with WPP and SPP and becomes higher relative to threshold THI1 but remains lower relative to threshold THI2. Hence, this event has included in the category of Islanding events.

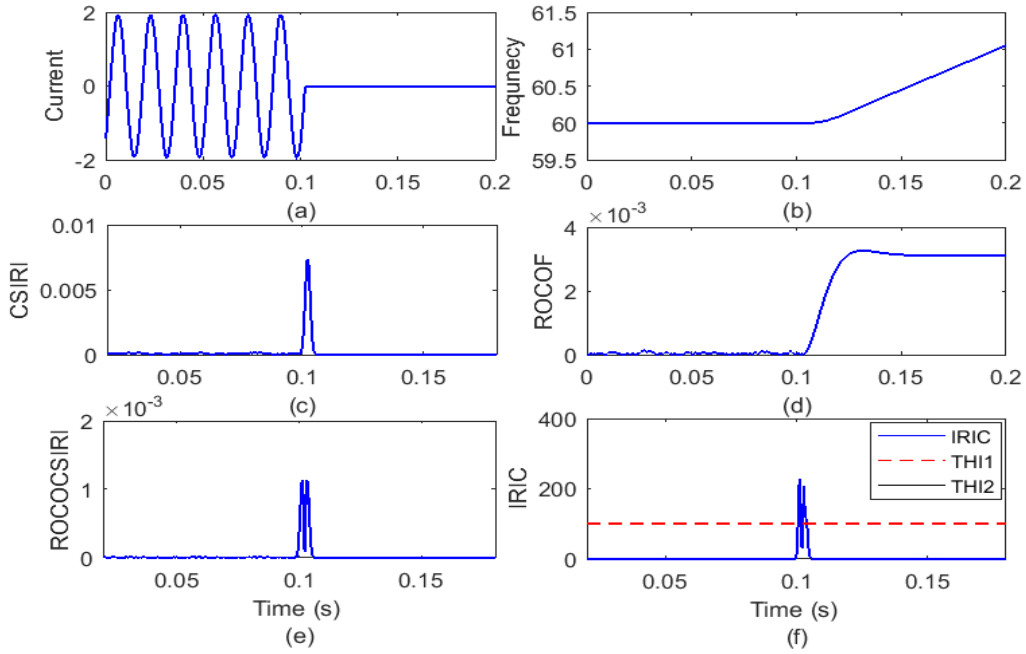

Figure 4. Islanding with WPP and SPP (a) current (b) frequency (c) CSIRI (d) ROCOF (e) ROCOCSIRI (f) IRIC.

C. Islanding with availability of WPP

Test distribution grid having WPP & SPP is simulated for 0.2 s and WPP is kept disconnected from network. Islanding event is simulated at 6th cycle in the presence of WPP by disconnecting test distribution system from utility grid network. Current waveform and frequency are recorded at junction 650 of grid and explained in Figure 5 (a) & (b) sequentially. Proposed CSIRI, ROCOF, ROCOCSIRI and IRIC are detailed Figure 5 (c), (d), (e) and (f) respectively.

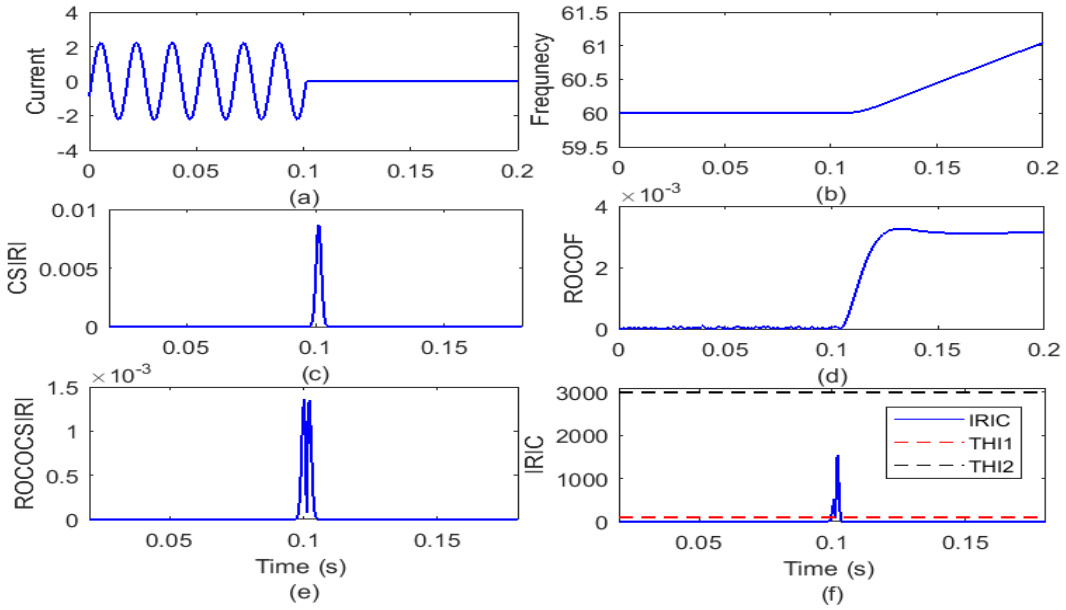

Figure 5. Islanding with WPP (a) current (b) frequency (c) CSIRI (d) ROCOF (e) ROCOCSIRI (f) IRIC.

Figure 5 (a) depicts that current has reduced to zero at instant of occurrence of islanding with WPP. Figure 5 (b) describes that frequency increases due to occurrence of islanding with WPP. Magnitude of CSIRI index has increased with sharp peak at instant of islanding and retained low values for all other times as detailed in Figure 5 (c). Figure 5 (d) details that ROCOF is nearly zero prior to occurrence of islanding and raised just after occurrence of islanding. Figure 5 (e) also describes that magnitude of the ROCOCSIRI has increased with high magnitude peak and low for all other times. Figure 5 (f) details that magnitude of IRIC has increased due to occurrence of islanding with WPP and attains high values relative to threshold THI1 but retains values lower relative to threshold THI2. Hence, this event has included in the category of Islanding events.

D. Islanding with SPP

Test distribution grid having WPP & SPP is simulated for 0.2 s and SPP is not integrated to grid. Islanding event is simulated at 6th cycle in the presence of SPP by disconnecting test distribution system from utility grid network. Current waveform and frequency are recorded at junction 650 of grid and explained in Figure 6 (a) & (b) sequentially. Proposed CSIRI, ROCOF, ROCOCSIRI and IRIC are detailed in Figure 6 (c), (d), (e) and (f) sequentially.

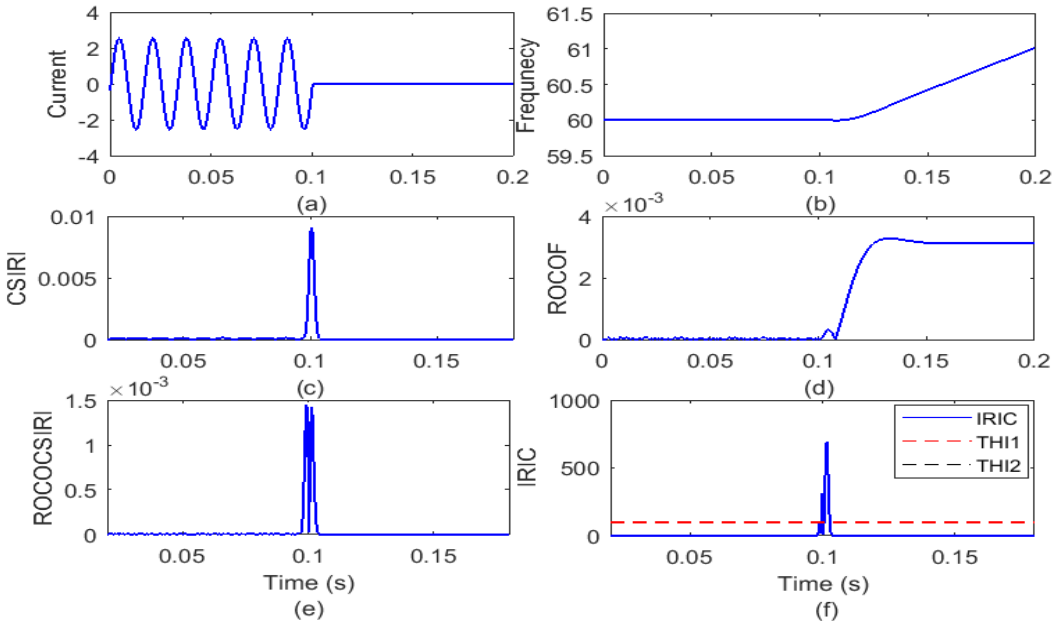

Figure 6. Islanding with SPP (a) current (b) frequency (c) CSIRI (d) ROCOF (e) ROCOCSIRI (f) IRIC.

Figure 6 (a) depicts that current reduced to zero due to occurrence of islanding with WPP. Figure 6 (b) describes that frequency increases due to occurrence of islanding with SPP. Magnitude of CSIRI index has increased with sharp peak at instant of islanding and retains low values for all other times as detailed in Figure 6 (c). Figure 6 (d) details that ROCOF is nearly zero prior to occurrence of islanding and rises just after occurrence of islanding with SPP. Figure 6 (e) also describes that magnitude of the ROCOCSIRI has increased with high magnitude peak and low for all other times. Figure 6 (f) details that magnitude of IRIC has increased due to occurrence of islanding with SPP and becomes high relative to threshold THI1 but remains lower values relative to threshold THI2. Hence, this event has included in the category of Islanding events.

E. Line to ground fault

Test distribution grid having WPP & SPP is simulated for 0.2 s. Line to ground (LG) fault event is simulated at 6th cycle on junction 646 of distribution grid at 0.1 s. This LG fault event involves the phase-A and ground. Fault resistance, ground resistance, snubber resistance and snubber capacitance equal to 0.001 Ω, 0.01 Ω, 10^6 Ω and infinity respectively are used to simulate the line to ground fault. Current waveform and frequency are recorded at junction 650 of grid and explained in Figure 7 (a) and (b) sequentially. Proposed CSIRI, ROCOF, ROCOCSIRI and IRIC are detailed in Figure 7 (c), (d), (e) and (f) respectively.

Figure 7 (a) depicts that current magnitude has increased to zero at instant of occurrence of LG fault on the test distribution system. Figure 7 (b) describes that frequency oscillates after occurrence of LG fault for a certain period of time and subsequently tries to settle near 60 Hz. Magnitude of CSIRI index has increased with sharp magnitude peak at instant of occurrence of LG fault and remains low for all other times as detailed in Figure 7 (c). Figure 7 (d) details that ROCOF is nearly zero prior to occurrence of islanding and raised just after occurrence of LG fault and ripples are observed till the frequency variations persist. Figure 7 (e) also describes that magnitude of the ROCOCSIRI has increased with high magnitude peak and low for all other times. Figure 7 (f) details that magnitude of IRIC has increased due to occurrence of LG fault and become higher than the threshold THI2. Hence, this event has been included in the category of fault events which is non-islanding event.

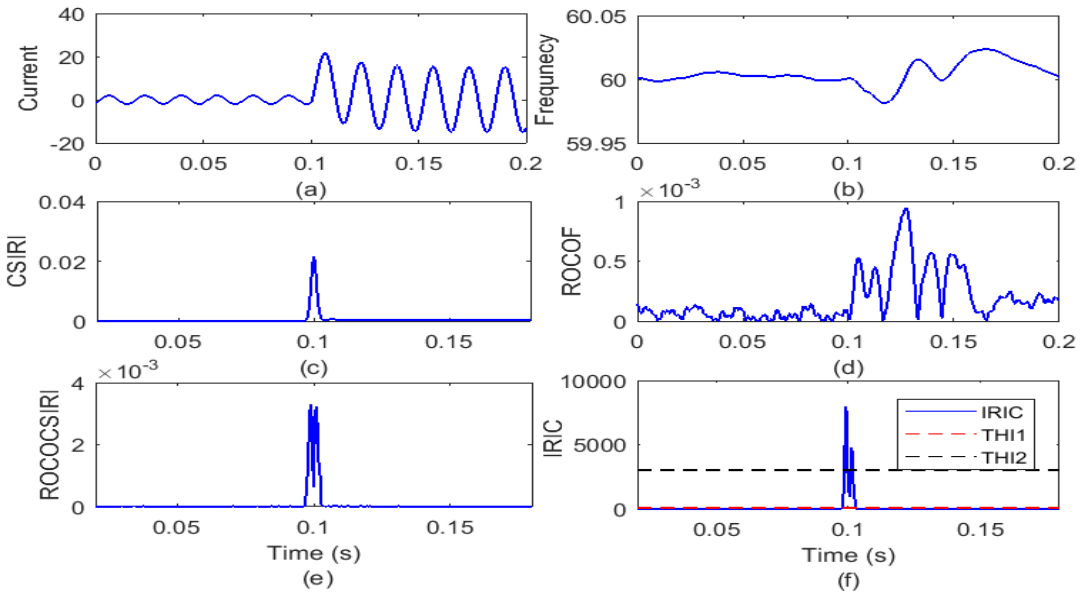

Figure 7. Line to ground fault (a) current (b) frequency (c) CSIRI (d) ROCOF (e) ROCOCSIRI (f) IRIC.

F. Line to line fault

Test distribution grid having WPP & SPP is simulated for 0.2 s. Line to line (LL) fault event is simulated at 6th cycle on junction 646 of distribution grid. Current waveform and frequency are recorded at junction 650 of grid and explained in Figure 8 (a) and (b) respectively. Proposed CSIRI, ROCOF, ROCOCSIRI and IRIC are detailed in Figure 8 (c), (d), (e) and (f) respectively.

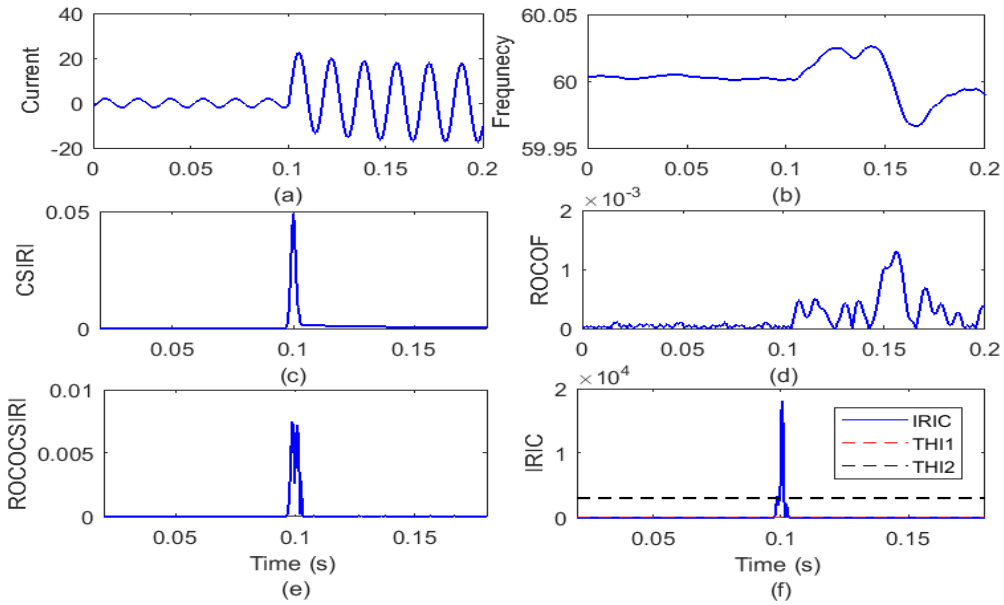

Figure 8. Line to line fault (a) current (b) frequency (c) CSIRI (d) ROCOF (e) ROCOCSIRI (f) IRIC.

Figure 8 (a) depicts that current magnitude has increased at instant of occurrence of LL fault on distribution system. Figure 8 (b) describes that frequency oscillates due to occurrence of LL fault and after a certain period of time it tries to settle near 60 Hz. Magnitude of the CSIRI index has increased with sharp magnitude peak at instant of occurrence of LL fault and remains low for all other times as detailed in Figure 8 (c). Figure 8 (d) details that ROCOF is nearly zero prior to occurrence of islanding and raised just after occurrence of LL fault and ripples are observed till the frequency variations persist. Figure 8 (e) also describes that magnitude of the ROCOCSIRI has increased with high magnitude peak and low for all other times. Figure 8(f) details that magnitude of IRIC has increased due to occurrence of LL fault and become higher than the threshold THI2. Hence, this event has been included in the category of fault events which is non-islanding event.

G. Double line to ground fault

Test distribution grid having WPP & SPP is simulated for 0.2 s. Double line to ground (LLG) fault event is simulated at 6^{th} cycle on junction 646 of distribution grid. Current waveform and frequency are recorded at junction 650 of grid and explained in Figure 9 (a) and (b) sequentially. Proposed CSIRI, ROCOF, ROCOCSIRI and IRIC are detailed in Figure 9 (c), (d), (e) and (f) respectively.

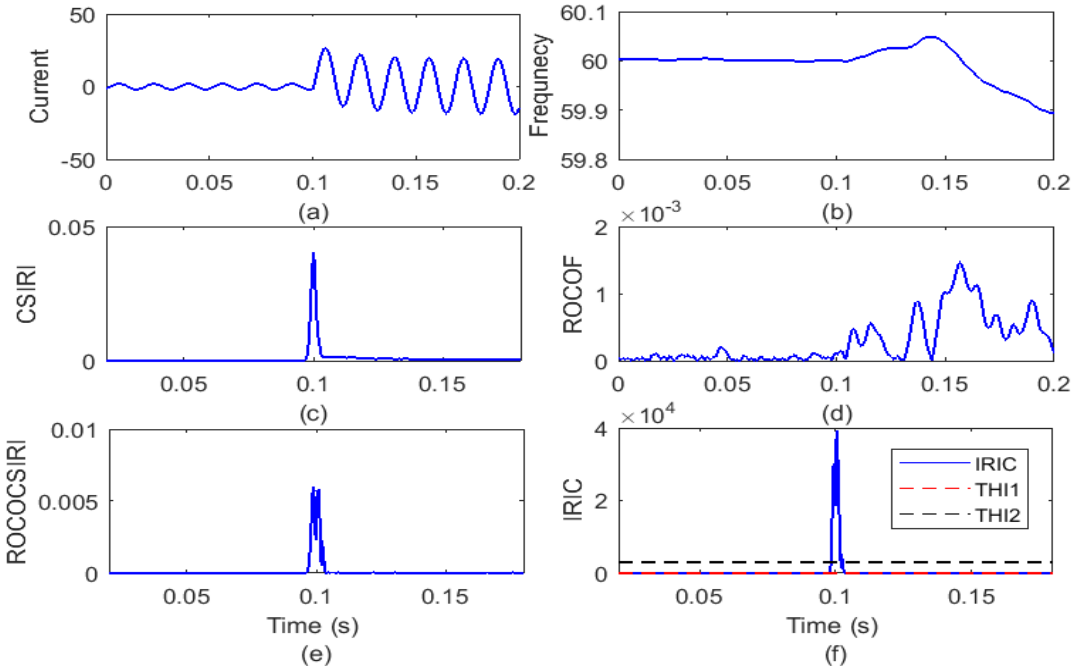

Figure 9. LLG fault (a) current (b) frequency (c) CSIRI (d) ROCOF (e) ROCOCSIRI (f) IRIC.

Figure 9 (a) depicts that current magnitude has increased at instant of occurrence of LLG fault on test distribution system. Figure 9 (b) describes that frequency decreases after incidence of the LLG fault for a certain period of time and it tries to settle near 60 Hz. Magnitude of the CSIRI index has increased with sharp magnitude peak at instant of occurrence of LLG fault and remains low for all other times as detailed in Figure 9 (c). Figure 9 (d) details that ROCOF is nearly zero prior to occurrence of LLG fault event and increases just after incidence of the LLG fault event and ripples are observed till the frequency variations persist. Figure 9 (e) also describes that magnitude of the ROCOCSIRI has increased with high magnitude peak and low for all other times. Figure 9 (f) details that magnitude of IRIC has increased due to occurrence of LLG fault, which gains higher values relative to threshold THI2. Hence, this event has been included in the category of fault events which is non-islanding event.

H. Three phase fault involving ground

Test distribution grid having WPP & SPP is simulated for 0.2 s. Three phases to ground (LLG) fault event is simulated at 6th cycle on node 646 of test distribution grid. Current waveform and frequency are recorded at junction 650 of grid and explained in Figure 10 (a) and (b) sequentially. Proposed CSIRI, ROCOF, ROCOCSIRI and IRIC are detailed Figure 10 (c), (d), (e) and (f) respectively.

Figure 10 (a) depicts that current has risen at instant of occurrence of LLLG fault on distribution system. Figure 10 (b) describes that frequency first increases and subsequently decreases after incidence of LLLG fault. Magnitude of the CSIRI index has increased with sharp magnitude peak at instant of occurrence of LLLG fault and remains low for all other times as detailed in Figure 10 (c). Figure 10 (d) details that ROCOF is nearly zero prior to occurrence of LLLG fault and raised just after occurrence of LLLG fault and ripples are observed till the frequency variations persist. Figure 10 (e) also describes that magnitude of the ROCOCSIRI has increased with high magnitude peak and

low for all other times. Figure 10 (f) details that the magnitude of IRIC has increased due to occurrence of LLG fault, which attains high values relative to threshold THI2. Hence, this event has been included in the category of fault events which is non-islanding event.

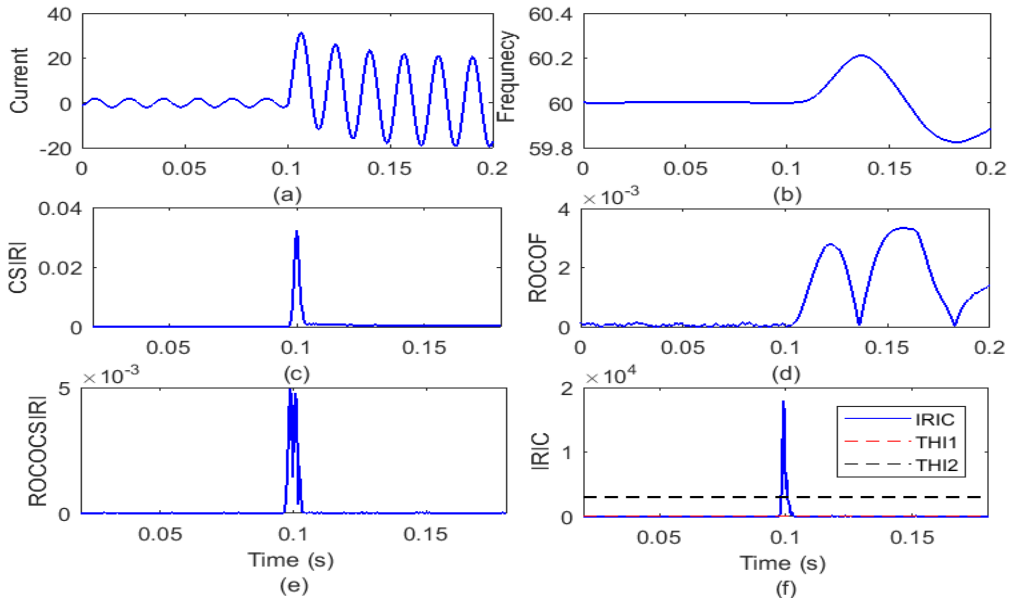

Figure 10. Three phase fault involving ground (a) current (b) frequency (c) CSIRI (d) ROCOF (e) ROCOCSIRI (f) IRIC.

I. Load switching

Test distribution grid interfaced with WPP & SPP is simulated for 0.2 s. Load consisting of 843 kW & 462 kVAr and integrated on junction 675 is switched off at 4th cycle and again switched on at 6th cycle after start of simulation. Current waveform and frequency are recorded at junction 650 of grid and detailed in Figure 11 (a) and (b) sequentially. Proposed CSIRI, ROCOF, ROCOCSIRI and IRIC are detailed in Figure 11 (c), (d), (e) and (f) sequentially.

Figure 11 (a) depicts that current decreases at instant of load switching off and regains value at instant of switching on the load. Figure 11 (b) describes that frequency increases at instant of load switching off and decreased at instant of load switching on. After short time duration of load switching off/on event the frequency attains normal value of 60 Hz. Magnitude of the CSIRI index has increased with sharp magnitude peaks at instant of occurrence of load switching off/on and remains low for all other times as detailed in Figure 11 (c). Figure 11 (d) details that ROCOF is nearly zero prior to occurrence of load switching off and increases just after occurrence of load switching off event and ripples are observed till the frequency variations persist. Similar, phenomenon is perceived at instant of load switching on. Figure 11 (e) also describes that magnitude of the ROCOCSIRI has increased with low value peak at instant of load switching off/on and low for all other times. Figure 11 (f) details that the magnitude of IRIC has increased with peak of low value at instant of load switching off/on but remains lower compared to threshold THI1. Hence, this event has been included in the category of fault events which is non-islanding event of operational event.

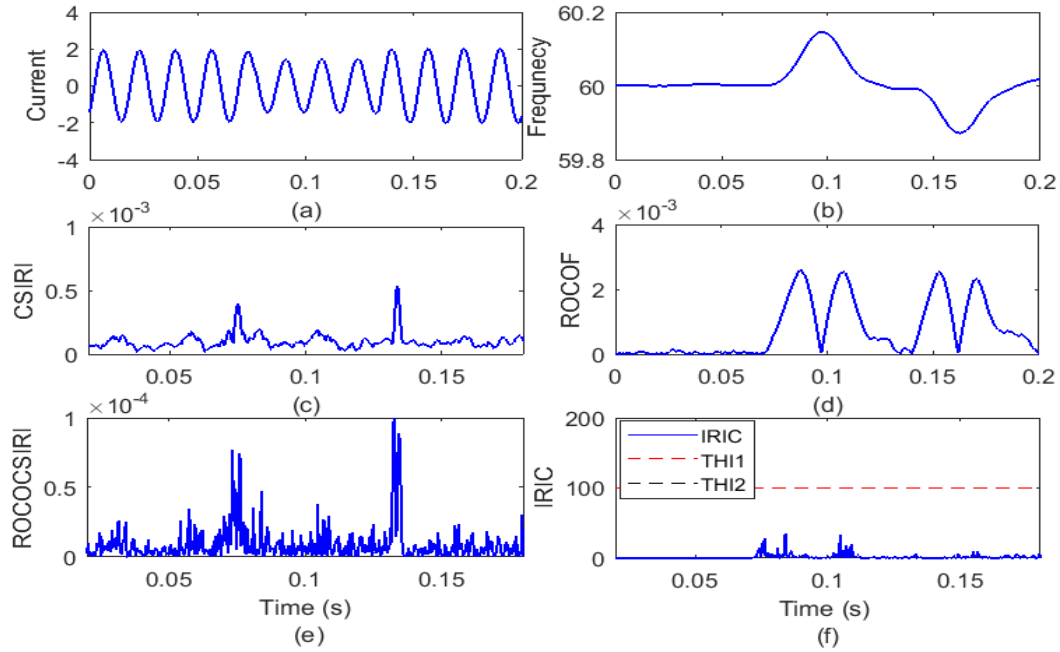

Figure 11. Condition of load switching (a) current (b) frequency (c) CSIRI (d) ROCOF (e) ROCOCSIRI (f) IRIC.

J. Outage of wind generator

Test distribution grid having WPP & SPP is simulated for 0.2 s. WPP integrated on junction 680 is disconnected at 6th cycle. Current waveform and frequency are recorded at junction 650 of test network. Proposed CSIRI, ROCOF, ROCOCSIRI and IRIC are computed. It is perceived that IRIC has increased and also has low value peak at WPP outage instant but remains lower compared to threshold THI1. Hence, this event has been included in the category of operational events which is non-islanding event of operational event.

H. Outage of solar PV generator

Test distribution grid having WPP & SPP is simulated for 0.2 s. SPP integrated on junction 680 is disconnected at 6th cycle. Current waveform and frequency are recorded at junction 650 of test network and CSIRI, ROCOF, ROCOCSIRI & IRIC are computed. It is inferred that IRIC has increased and has a small peak value at time of SPP outage but remains lower compared to threshold THI1. Hence, this event has been included in the category of operational events which is non-islanding event of operational event.

5. Event classification

Islanding scenarios have been classified from fault scenarios and operational conditions applying simple decision rules. Peak magnitude of the IRIC is considered as the key factor for the decision rules. Peak of IRIC for different events is tabulated in Table 1. Threshold magnitudes THI1 and THI2 have been set equal to 100 and 3000 respectively to differentiate the events. Event classification is illustrated in Figure 12. It is perceived that various events are categorized one by one. Condition IRIC > THI2, indicates presence of events with faulty nature. Further, condition

IRIC < THI1 indicates the operational events. The islanding events are recognized of condition THI1 < IRIC < THI2 is fulfilled.

Table 1. Peak of current supported IRI.

S. No.	Event Type	Peak of IRIC
1	Healthy scenario without any disturbance	4.87
2	Islanding with WPP and SPP	228.69
3	Islanding with WPP	1789.10
4	Islanding with SPP	705.47
5	LG fault	7800.96
6	LL fault	18230
7	LLG fault	39810
8	LLLG fault	18421
9	Load Switching	19.45
10	Outage of Wind Generator	54.68
11	Outage of Solar PV Generator	17.14

6. Performance comparison study

Proposed current based IDM is effective for recognizing the islanding in time interval smaller than 0.05 cycle. However, an IDM using rate of change of voltage (ROCOV) & ROCOF and Wavelet transform (WT) detect islanding condition in time-interval which varies from 0.25 to 0.5 cycles [20,21]. Hence, IDM designed in this manuscript is fast and has high accuracy in comparison to the IDMs reported in [20,21]. In [22], a Slantlet transform and ridgelet probabilistic neural network (RPNN) based IDM is proposed to detect islanding events and discriminate these events from the switching events and power quality disturbances. In paper [22], IDM is not tested to discriminate the faulty events from the islanding events which is the critical limitation the IDM. The IDM proposed in this paper is also effective to discriminate the faulty events from the islanding events.

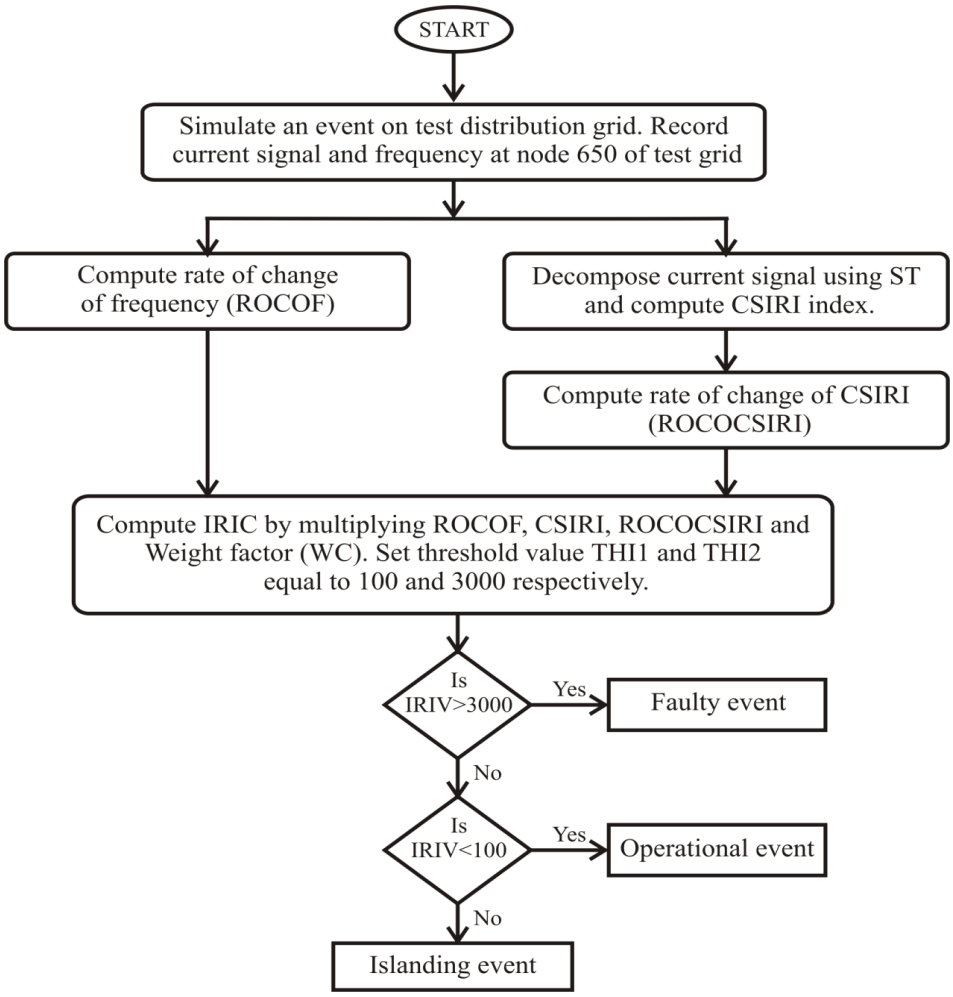

Figure 12. Event classification.

7. Concluding remarks

An algorithm supported by current signals and ROCOF is introduced in this paper to identify the islanding events. Current is decomposed applying ST at 3.84 kHz SF and CSIRI is computed. Rate of change of CSIRI (ROCOCSIRI) is computed. Proposed current based islanding recognition index (IRIC) is computed by multiplication of ROCOF, CSIRI, ROCOCSIRI and a WC. Threshold values THI1 and THI2 are selected as 100 and 3000 for IRIC for identifying the Islanding conditions and also for differentiating these conditions from non-islanding events which include both the faulty and operational conditions. Magnitude of IRIC is greater than the 3000 for the faulty events and lowers than 100 for operational events. For the islanding events, magnitude of IRIC falls in between the 100 and 3000. It is concluded that the events have been grouped in three categories which are islanding, faulty and operational conditions effectively. Hence, islanding conditions are classified effectively in the islanding and non-islanding events. Performance of the proposed IDM is compared with the IDMs using Wavelet transform, rate of change of voltage Slantlet transform and ridgelet probabilistic neural network reported in literature and it is established that proposed IDM performance better considering certain dimensions. Experimental validation of the results may be considered as future scope of research work.

Conflict of interest

There is no conflict of interest of any author in any form.

References

1. Kaushik R, Mahela OP, Bhatt PK, et al. (2020) Recognition of Islanding and Operational Events in Power System with Renewable Energy Penetration Using a Stockwell Transform Based Method. *IEEE Syst J*. https://doi.org/10.1109/JSYST.2020.3020919
2. Mahela OP, Sharma Y, Ali S, et al. (2021) Voltage Based Hybrid Algorithm using Parameter Variations and Stockwell Transform for Islanding Detection in Utility Grids. *Informatics* 8: 21. https://doi.org/10.3390/informatics8020021
3. Mahela OP, Garg AR, Khan B, et al. (2020) Combined Stockwell and Hilbert Transforms Based Technique for the Detection of Islanding Events in Hybrid Power System. *46th Annual Conference of the IEEE Industrial Electronics Society (IES), IECON 2020*, October 18-21, Singapore. https://doi.org/10.1109/IECON43393.2020.9254764
4. Mahela OP, Gupta R, Khan B, et al. (2020) A Voltage Based Algorithm Using Combined Features of Stockwell Transform and Hilbert Transform for Detection of Islanding Events. *2020 IEEE International Conference on Environment and Electrical Engineering*, University of Rome "Sapienza" and University of Madrid "Carlos III", Madrid, Spain. https://doi.org/10.1109/EEEIC/ICPSEurope49358.2020.9160551
5. Pedrino EC, Yamada T, Lunardi TR, et al. (2019) Islanding detection of distributed generation by using multi-gene genetic programming based classifier. *Applied Soft Computing Journal*, 74: 206–215. https://doi.org/10.1016/j.asoc.2018.10.016
6. Reddy JR, Pandian A, Reddy CR (2020) An efficient learning based RFMFA technique for islanding detection scheme in distributed generation systems. *Applied Soft Computing Journal* 96: 106638. https://doi.org/10.1016/j.asoc.2020.106638
7. Raza S, ur Rahman T, Saeed M, et al. (2020) Performance analysis of power system parameters for islanding detection using mathematical morphology. *Ain Shams Eng J* 12: 517–527. https://doi.org/10.1016/j.asej.2020.07.023
8. Thomas SR, Kurupath V, Nair U (2020) A passive islanding detection method based on K-means clustering and EMD of reactive power signal. *Sustain Energy Grids* 23: 100377. https://doi.org/10.1016/j.segan.2020.100377
9. Khamis A, Shareef H, Bizkevelci E, et al. (2013) A review of islanding detection techniques for renewable distributed generation systems. *Renew Sust Energ Rev* 28: 483–493. https://doi.org/10.1016/j.rser.2013.08.025
10. Funabashi T, Koyanagi K, Yokoyama R (2003) A Review of Islanding Detection Methods for Distributed Resources. *2003 IEEE Bologna PowerTech Conference*, June 23-26, Bologna, Italy.
11. Khan MA, Haque A, Kurukuru VB, et al. (2022) Islanding detection techniques for grid-connected photovoltaic systems-A review. *Renew Sust Energ Rev* 154: 111854. https://doi.org/10.1016/j.rser.2021.111854
12. Mobashsher MM, Keypour R, Savaghebi M (2021) Distributed optimal voltage control in islanded microgrids. *Int T Electr Energy* 31: e13045. https://doi.org/10.1002/2050-7038.13045

13. Isazadeh A, Adabi J, Rezanejad M, et al. (2021) Operation and Control of a Grid-Connected Asymmetrical Cascaded Multilevel Inverter. *IEEE J Em Sel Top P* 9: 1614–1623. https://doi.org/10.1109/JESTPE.2020.2991385
14. Ram Ola S, Saraswat A, Goyal SK, et al. (2020) Alienation Coefficient and Wigner Distribution Function Based Protection Scheme for Hybrid Power System Network with Renewable Energy Penetration. *Energies* 13: 1120. https://doi.org/10.3390/en13051120
15. Mahela OP, Shaik AG (2015) Power quality detection in distribution system with wind energy penetration using discrete wavelet transform. In: *2nd IEEE International Conference on Advances in Computing and Communication Engineering (ICACCE-2015)*, Tula's Institute, Dehradun, India. https://doi.org/10.1109/ICACCE.2015.52
16. Mahela OP, Shaik AG (2015) Detection of power quality disturbances associated with grid integration of 100 kW solar PV plant. In: *1st IEEE Uttar Pradesh Conference-International Conference on Energy Economics and Environment (ICEEE 2015)*, Galgotia Institute of Engineering and Technology, Noida, India. https://doi.org/10.1109/EnergyEconomics.2015.7235070
17. Yogee GS, Mahela OP, Kansal KD, et al. (2020) An Algorithm for Recognition of Fault Conditions in the Utility Grid with Renewable Energy Penetration. *Energies* 13: 2383. https://doi.org/10.3390/en13092383
18. Kulshrestha A, Mahela OP, Gupta MK, et al. (2020) A Hybrid Protection Scheme Using Stockwell Transform and Wigner Distribution Function for Power System Network with Solar Energy Penetration. *Energies* 13: 3519. https://doi.org/10.3390/en13143519
19. Shaik AG, Mahela OP (2018) Power quality assessment and event detection in hybrid power system. *Electr Pow Syst Res* 161: 26–44. https://doi.org/10.1016/j.epsr.2018.03.026
20. Quoc-Tuan T (2016) New Methods of Islanding Detection for Photovoltaic Inverters. *2016 IEEE PES Innovative Smart Grid Technologies Conference Europe (ISGT-Europe)*, Ljubljana, Slovenia. https://doi.org/10.1109/ISGTEurope.2016.7856317
21. Sharma R, Singh P (2012) Islanding Detection and Control in Grid Based System Using Wavelet Transform. *2012 IEEE Fifth Power India Conference*, Murthal, India. https://doi.org/10.1109/PowerI.2012.6479557
22. Ahmadipour M, Hizam H, LutfiOthman M, et al. (2019) Islanding detection method using ridgelet probabilistic neural network in distributed generation. *Neurocomputing* 329: 188–209. https://doi.org/10.1016/j.neucom.2018.10.053

AIMS Press